

**SULFATE-CEMENTED SOILS DETECTED IN TES DATA THROUGH THE APPLICATION OF AN AUTOMATIC BAND DETECTION ALGORITHM.** A. Gendrin<sup>1</sup>, J. F. Mustard<sup>2</sup>, <sup>1</sup>Institut d'Astrophysique Spatiale, CNRS, Université Paris 11, bâtiment 121, 91405 Orsay Campus, France [aline.gendrin@ias.fr](mailto:aline.gendrin@ias.fr), Department of Geological Science, Box 1846, Brown University, Providence RI, 02912 John\_Mustard@brown.edu.

**Introduction:** We apply an automatic band detection algorithm, based on the wavelet transform [1], to the TES dataset. This algorithm detects the wavelength positions of bands in spectra and then classifies together spectra with similar absorption band positions. Using this algorithm we show that an absorption band at  $1120\text{ cm}^{-1}$  is systematically present in spectra corresponding to the regions of high sulfate concentration according to [2]. This result addresses again the question of the detectability of cemented sulfates in TES dataset, despite the low concentration resulting from the application of a linear unmixing method.

Elemental sulfur was identified in the Martian soil by the Viking and Pathfinder landers, in relatively high concentrations (~5-9 %) [3, 4, 5]. These landers also revealed that the soil was indurated in places. Comparative measurements in the indurated and normal soil showed that the concentration of sulfates is higher in the indurated soil. These observations led to the hypothesis that the duricrust on Mars contains cemented sulfates [4, 6, 7].

Cooper and Mustard [8] investigated the spectral characteristics of sulfates in the near and mid-infrared. They concluded that sulfate on Mars should be detectable by TES only if they form coherent surfaces via cementation. Cooper and Mustard [9] analyzed the TES dataset using an image-based linear unmixing and identified sulfate-cemented soils primarily in equatorial regions of intermediate albedo. This location agrees with previously hypothesized duricrust deposits [10, 11] though these did not have direct compositional evidence. Since the concentration of the identified sulfates does not reach the proposed 10% mineral abundance detection threshold [12] we propose to analyze the TES data with an independent approach to test the results of [9].

**Data processing:** We used the TES dataset, resampled as explained in Cooper and Mustard [2, 9]. These authors selected 8.5 millions of the best TES spectra, with appropriate viewing geometry, high temperature surface values, and high signal to noise ratios. They averaged the spectra so as to obtain a  $0.5^\circ \times 0.5^\circ$  gridded dataset.

We applied the automatic band detection algorithm based on the wavelet transform and described in [1]. The wavelet transform consists, in the way we use it, in the convolution of a wavelet with a spectrum. A wave-

let is an oscillating function with a zero mean and a finite energy. We show an example wavelet in fig 1.

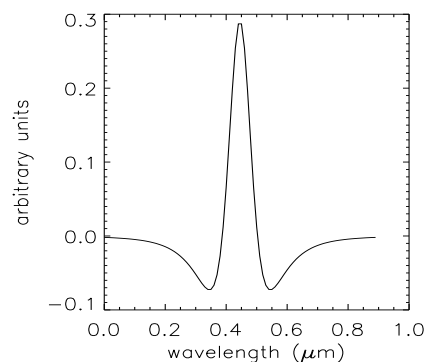


Fig 1: An example wavelet.

In our algorithm, we use the band pass filter property of the wavelet transform: the convolution of the wavelet with a spectrum creates a resonance at the location of an absorption band if the width of the wavelet is comparable to the width of the absorption band. Such a resonance creates a minimum at the band position, instead of the sometimes slight inflexion point corresponding to an absorption band. Since the wavelet transform is a band pass filter, it is also a low pass filter, and the noise is filtered, allowing us to focus on the absorption bands in the dataset. The band position we detect is actually the band barycentre which may be offset relative to the real band centre. This property makes our algorithm sensitive to the shape of the bands, which is an advantage.

We apply the wavelet transform on each spectrum of the dataset, and identify, for each resulting filtered spectrum, the minima, which correspond to the band positions. We obtain a set of band positions for each spectrum and classify together the spectra with bands at the same positions.

For the TES dataset, we use a wavelet of  $200\text{ cm}^{-1}$  wide, which is appropriate for the study of the sulfate, and type I and type II bands, since the wavelet must have a width comparable to the width of the bands in the dataset. We apply the wavelet transform in the  $1300\text{-}850\text{ cm}^{-1}$ , where the main absorptions of these minerals are located.

**Results:** The resulting classification is presented in Fig. 2. We first observe that the classification identifies the compositional difference existing between type I

and type II terrains, at locations in agreement with [13]. As expected, the band barycentre for type I terrain is located at slightly shorter wavenumbers than for type II terrain: type I terrain corresponds to the two classes with mean band barycenters at 1055 and 1065  $\text{cm}^{-1}$ , and type II corresponds to the two classes at 1075 and 1085  $\text{cm}^{-1}$ . The subdivision of type I in two classes (the same is true for type II) corresponds to different concentrations of the material. For example, the subclass of type II with a mean band barycentre at 1065  $\text{cm}^{-1}$ , roughly corresponds to the regions appearing in red in the type I map in [13]. This means that this class corresponds to the highest concentrations of type I.

The classification identifies several unique classes in bright regions. These classes are well grouped spatially indicating that random noise does not dominate the classification. The classification defines a dichotomy between the near-equatorial orange/reddish classes, and the yellow/green classes that are more polar. The orange/reddish region occupies the Martian regions where Cooper and Mustard [2] identified cemented sulfates. Our independent method shows that the composition of the sulfate rich regions identified by [2] is homogeneous. The mean position of the identified band, located at  $\sim 1120 \text{ cm}^{-1}$ , is consistent with the position of the 5%  $\text{MgSO}_4$  crust band hypothesized by [9]. Moreover, the band centers of the other classes in the bright regions are located at lower wavenumbers (mainly 1050-1070  $\text{cm}^{-1}$ ).

**Conclusion:** Our analysis of the TES dataset using a band detection algorithm based on the wavelet trans-

form [1] identifies bright regions with distinct absorption bands consistent with the Restrahlen band of 5%  $\text{MgSO}_4$ -cemented soil [8]. The location of these regions is consistent with the regions identified by Cooper and Mustard [2] as rich in sulfate-cemented soils.

While we, nor [2], provide estimates of sulfate abundance, the maximum possible is on the order of 5%. This 5% abundance of sulfate is below the 10% concentration needed to ascertain the presence of a mineral in TES spectra [12]. However, two independent methods of analysis [1, 2], identify cemented sulfates [2] or a band consistent with cemented sulfates [1] in the same regions on Mars. Consequently, the work presented here provides support for the conclusions formulated in [2].

**References:** [1] Gendrin and Erard (2003) *LPSC XXXIV*, #1376. [2] Cooper and Mustard (2001) *LPSC XXXII*, #2048. [3] Toulmin P. et al. (1997) *JGR* **84**, 4625-4634 [4] Clark, B.C. et al. (1982) *JGR* **87**, 10059-10067 [5] Rieder R. et al. (1997) *Science* **278**, 1771-1774 [6] Baird A.K. et al. (1977) *JGR* **82**, 4595-4624 [7] Clark, B.C. (1993) *GCA* **57**, 4575-4581. [8] Cooper and Mustard (2002) *Icarus* **158**, 42-55. [9] Cooper and Mustard (2002), *LPSC XXXIII*, #1997. [10] Murchie et al. (2000) *Icarus* **147**, 441-471. [11] Arvidson R.E. et al. (1994) *JGR*, **94**, 1573-1574. [12] Bandfield et al. (2002) *JGR* **107**, 9-1. [13] Bandfield et al. (2000) *Science* **287**, 1626-1630.

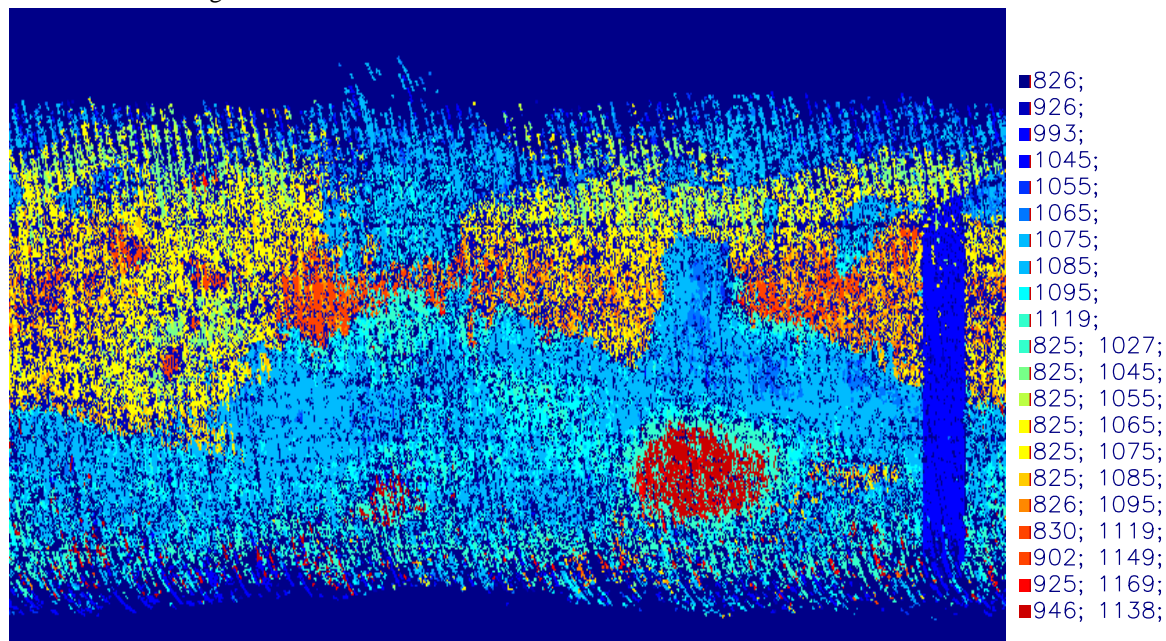


Fig 2: TES classification based on band positions detected with a wavelet algorithm. Mean band positions for each class shown on the right.